Available online at www.sciencedirect.com

ScienceDirect

Procedia Structural Integrity 17 (2019) 632–642

Structural Integrity Procedia

www.elsevier.com/locate/procedia

ICSI 2019 The 3rd International Conference on Structural Integrity

Assessment of the Mechanical Integrity of a 2 mm AA6060-T6 Butt Weld Produced Using the Hybrid Metal Extrusion & Bonding (HYB) Process – Part II: Tensile Test Results

Lise Sandnes[a,*], Luca Romere[b], Øystein Grong[a,c], Filippo Berto[a], Torgeir Welo[a]

[a]*Department of Mechanical and Industrial Engineering, Norwegian University of Science and Technology, Richard Birkelands vei 2b, 7491 Trondheim, Norway*

[b]*Department of Management and Engineering, University of Padua, Stradella San Nicola 3, 36100 Vicenza, Italy*

[c]*HyBond AS, NAPIC, Richard Birkelands vei 2b, 7491 Trondheim, Norway*

Abstract

The present investigation is concerned with solid state butt welding of 2 mm thin AA6060-T6 profiles at room temperature (RT), using the HYB process and AA6082-T4 as filler material (FM). In Part II of this investigation the tensile properties of the butt weld have been evaluated as a follow-up of the three-point bend testing done in Part I. In the HYB case the weld can be sub-divided into two distinct zones, i.e. the Extrusion Zone (EZ) and the Heat-Affected Zone (HAZ). The EZ, which is a composite material consisting of a mix of a strong FM and a soft HAZ material, displays superior tensile properties compared to the HAZ. By allowing for this in the subsequent finite element (FE) simulations of the load-bearing capacity of the joint, the observed stress-strain response of the HYB weld has been fully reproduced and rationalized. These results show that the tensile properties are comparable with those reported for FSW of 2 mm AA6082-T6 profiles and surpass those reported for FSW of 2 mm 6061-T6 profiles as far as the yield strength is concerned.

Peer-review under responsibility of the ICSI 2019 organizers.

Keywords: Hybrid Metal Extrusion & Bonding (HYB); solid state joining; filler metal addition; thin aluminum profiles; tensile testing.

1. Introduction

Al-Mg-Si alloys are to an increasing extent used for structural applications within the transportation and automotive sector by virtue of their high strength, excellent formability, low weight and good resistance to general corrosion

* Corresponding author. Tel.: +47 924 66 968.
E-mail address: lise.sandnes@ntnu.no

2452-3216
Peer-review under responsibility of the ICSI 2019 organizers.
10.1016/j.prostr.2019.08.085

(Davis, 1993, Hirsch, 2011). In load-bearing structures the solute-rich AA6082 and AA6061 variants are most commonly employed, since they provide the highest specific strength (i.e. yield strength to density ratio) in the peak-aged (T6) temper condition (Hatch, 1984). However, problems arise when these alloys following peak-ageing are subjected to welding, as frequently done in industrial manufacturing of aluminum components (Grong, 1997, Hirsch, 2011). This is because T6 heat-treated Al-Mg-Si alloys are particularly prone to Heat-Affected Zone (HAZ) softening after Gas Metal Arc Welding (GMAW) and Friction Stir Welding (FSW), which reduces the load-bearing capacity of the entire assembly (Frigaard *et al.*, 2001, Myhr and Grong, 2009). In addition, welding of thin section aluminum plates and profiles creates additional problems related to buckling and global distortions (Zha and Moan, 2001, Bruce and Eyres, 2012). These problems are most severe in GMAW, but can be reduced by the use of an energy efficient solid state process like FSW (Kumar *et al.*, 2008, Farajkhah *et al.*, 2017, Ma *et al.*, 2018). Still, buckling and distortions represent a great challenge for many manufacturers of aluminum parts, who daily face the strict dimensional tolerance requirements being enforced by their customers.

No simple actions can be undertaken to counteract the negative effects of welding in thin section products. But a bold, new approach could be to instead select a lean aluminum alloy (e.g. of the 6060-T6 type), and employ this, in combination with solid state joining, for manufacturing of such products. The use of an aluminum alloy with a low base metal (BM) strength will inevitably reduce the significance of the HAZ softening. This is because the drop in strength following dissolution of the BM hardening precipitates will be correspondingly small. However, since FSW of thin plates may result in insufficient material feeding and consequently to undercuts and weld defects (Wanjara *et al.*, 2013, Huang *et al.*, 2016), an alternative solid state process enabling filler metal addition should be aimed at. If the resulting mechanical properties and dimensional tolerances achieved in the as-welded condition matches or surpass those obtained following GMAW and FSW of the high strength AA6082-T6 and AA6061-T6 variants, the approach is deemed to be viable and sound.

Recently, it has been documented that the Hybrid Metal Extrusion & Bonding (HYB) process can produce sound 4 mm thick AA6082-T6 butt welds using AA6082 filler metal additions with properties matching those of corresponding GMA and FS weldments (Sandnes *et al.*, 2018). Because the energy efficiency of the HYB method is comparable with that of FSW when it comes to heat input and extent of HAZ softening, this process should be an excellent candidate for butt welding of 2 mm thin AA6060-T6 extrusions. To meet the customer's dimensional tolerance requirements for manufacturing of wide profiles from narrow-width extrusions, both weld surfaces need to be slick as in FSW, without a reinforcement. At the same time as the joined profiles must be straight and display a nice surface finish in the as-welded condition.

In the preceding paper (Part I), the mechanical integrity of the 2 mm AA6060-T6 HYB joint was evaluated by means of visual inspection, metallographic examination and three-point bend testing (Sandnes *et al.*, 2019). In the as-welded condition, the 1000 mm long butt weld was seen to be straight and essentially free from global distortions and internal defects. However, during three-point bend testing root cracks did form on the retreating side of the joint because of "kissing" bond formation. Still, their appearance was not found to be devastating for the resulting mechanical integrity of the joint. This justifies further analyses and testing to unravel its entire mechanical performance and load-bearing capacity.

In the present paper (Part II) the main results from the transverse hardness measurements and the tensile testing are presented and analyzed. Finally, the results from the fatigue testing will be reported in an accompanying paper (Part III).

2. Experimental

The working principles of the HYB PinPoint extruder and its ability to handle different joint configurations and weld geometries as well as base metal combinations have been reported elsewhere (Sandnes *et al.*, 2018, Grong *et al.*, 2019, Grong *et al.*, 2019). For the 2 mm butt welding application, a stationary housing with no die opening at the rear for partial outlet of the extrudate is selected to prevent the formation of a reinforcement. When this closed housing is used in combination with a flat steel backing plate, a slick weld and root face can be obtained also in the HYB case as in FSW.

2.1. Materials and welding conditions

The 2 mm thin AA6060 extrusions used in the butt joining trial were received from an external supplier in the T6 temper condition. The other dimensions of the extrusions were 50 mm × 1000 mm. The filler material was a ϕ1.2 mm wire of the AA6082-T4 type produced by HyBond AS. The wire was made from a ϕ95 mm DC cast billet which then was homogenized, hot extruded, cold drawn and shaved down to the final dimension. The chemical compositions of the base and filler materials (BM and FM) are summarized in Table 1.

Table 1 Chemical compositions (wt.%) of the base and filler materials (BM and FM).

	Si	Mg	Cu	Fe	Mn	Cr	Zn	Ti	Zr	B	Other	Al
BM AA6060	0.483	0.435	-	0.176	0.038	-	0.036	0.021	-	-	0.078	Balance
FM AA6082	1.110	0.610	0.002	0.200	0.510	0.140	-	0.043	0.130	0.006	0.029	Balance

Prior to the welding operation, the two 1000 mm long extruded profiles were mounted in a fixture so that a 7.5 mm wide I-groove did form between them, as illustrated in Fig. 1(a). During butt welding the extruder head with its ϕ9 mm rotating cylindrical pin slides at a constant speed along the 7.5 mm wide I-groove, as shown in Fig. 1(b). Due to the synchronized spindle tip and pin rotation, the ϕ1.2 mm filler wire is continuously dragged by friction into and through the extrusion chamber. When it hits the abutment, the subsequent compression and pressure build-up eventually lead to extrusion of the plasticized aluminum in the axial direction through a set of moving dies in the rotating pin and downwards into the groove (Sandnes *et al.*, 2018). Because the pin diameter is larger than the groove width, the surface oxide being present at the groove walls becomes continuously mixed into the FM before bonding and consolidation occur behind the pin.

Table 2 summarizes the operational conditions employed in the butt welding operation. Note that the current combination of welding parameters used is not considered to be optimal, but represent rather a sensible compromise between a number of conflicting requirements to achieve a weld with the required groove filling and surface finish. A more in-depth analysis of the essential HYB process parameters and how they are interrelated are provided elsewhere (Grong *et al.*, 2019).

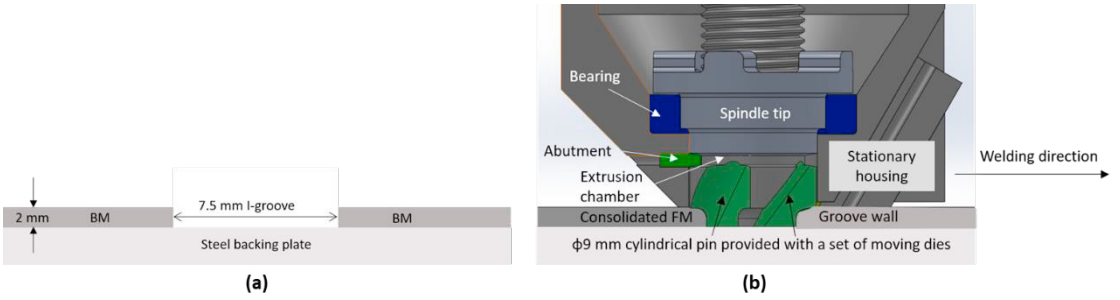

Fig. 1. Schematic and SolidWorks drawings highlighting the experimental set-up during butt welding of the 2 mm thin AA6060-T6 extruded profiles; (a) Transverse section showing the groove and base plate dimensions. (b) Longitudinal section through the extruder head and the weld with the rotating cylindrical pin in position within the groove and the closed stationary housing placed on the top.

Table 2. Operational conditions employed in the butt welding experiment with the 2 mm thin extruded profiles.

Pin rotation (RPM)	Travel speed (mm/s)	Wire feed rate (mm/s)	Gross heat input (kJ/mm)
250	8	122	0.28

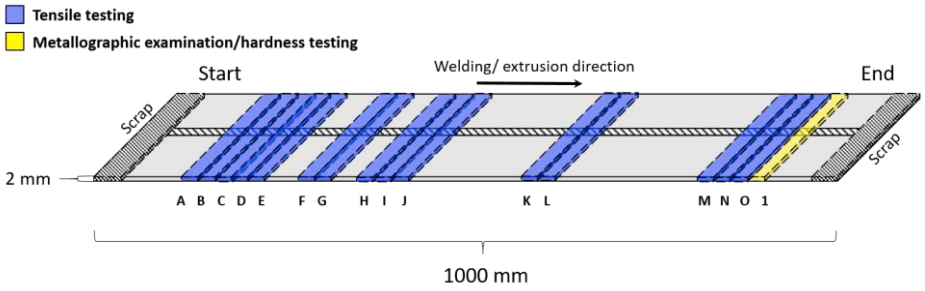

Fig. 2. Sketch showing the location and labelling of the different specimens used for metallographic examination (yellow) and tensile testing (blue) referred to the start position of the weld.

2.2. Metallographic examination

After the butt welding operation, one cross-sectional sample was cut from the end of the weld plate, as illustrated in Fig. 2, and made ready for metallographic examination using standard preparation techniques. In the present paper, only the results from the transverse hardness measurements at the end-position of weld are included. Additional optical images of the joint transverse macrostructure at different positions along the joint line are given in Part I (Sandnes *et al.*, 2019).

The hardness measurements were made in accordance to ASTM standard E92-16, using a Mitutoyo Micro Vickers hardness testing machine applying a constant load of 1 kg. The distance between each indentation was 0.5 mm. In total, three independent test series were carried out along the specimen horizontal mid-section. Finally, the base material hardness was established from twenty individual measurements being randomly taken on one separate specimen of the base plate.

Table 3. Overview of the specimens used for tensile testing. Included in the table are both their location and thickness, as well as the labelling and number of specimens tested. Note that the labelling is in accordance with that used in Fig. 2.

Weld zone tested		Specimen thickness (mm)	Labelling	Number of specimens tested
Extrusion zone	EZ	2	A, B, C	3
	EZ_{red}	1.8	H, I, J	3
Heat affected zone	HAZ	2	G, K, L	3
	HAZ_{red}	1.8	M, N, O	3
Base material	BM	2	D, E, F	3

2.3. Tensile testing

Two sets of tensile specimens were prepared for testing; one set having the original extrusion thickness of 2 mm, and another set having a reduced specimen thickness of 1.8 mm to remove the previously mentioned root defects due to “kissing” bond formation. For each specimen type, dual sets of tensile specimens were prepared. They have their center located either in the EZ or the HAZ on the retreating side (RS) of the weld. For the BM only 2 mm thick transverse tensile specimens were prepared for comparison with the weld samples. An overview of the specimen location, labelling and number of specimens being tested is given in Fig. 2 and Table 3.

The tensile testing was performed in accordance with ASTM standard E8/E8M-16a, using a MST Criterion electromechanical test machine (5 kN load cell) with a fixed cross-head speed of 0.3 mm/min. However, because of the limited extrusion profile dimensions, the subsize specimens used had a reduced section length and width of 18 and 4 mm, respectively and a total length of 64 mm, which is outside the standard specifications. This resulted in a grip section width and gauge length of 10 mm. Note that the short gauge length will affect the measured values for the

yield strength in cases where the extensometer does not fully sample the entire width of the soft HAZ. This issue will be fully addressed and commented on towards the end of the paper.

2.4. Finite element simulations

Simulations of the weld tensile test were conducted using the commercial finite element (FE) software code ABAQUS/CAE (6.17). In the ABAQUS mock-up the tensile specimen is modelled as a deformable object and presented by a solid mesh of 13680 linear brick elements (C3D8R). A finer mesh is chosen for the parallel length and curved parts of the specimen where most of the plastic deformation and stress concentration occur. The number of elements in the specimen thickness direction was set to 8 after conducting a mesh sensitivity analysis. Hence, mesh refinement above this point does not affect the resulting output data significantly.

3. Results

3.1. Transverse hardness profile

In Fig. 3 the HYB joint transverse hardness profile is presented together with the corresponding macrograph of the joint cross-section. In the plot each hardness point represent the mean value of three individual measurements, while the thin horizontal dotted line displays the average base material hardness (measured to be 84 HV). It follows from the figure that the hardness profile yields the characteristic W-shaped form, where the central part representing the EZ is relatively flat for about 8 mm, reaching an average hardness value of 67 HV. On each side of the EZ a drop in hardness is observed, which corresponds to the HAZ. The minimum HAZ hardness of 56 HV is observed on the RS of the joint about 5 mm from the weld center line. The total width of the weld zone (i.e. EZ + HAZ) is measured to be about 18 mm.

From the asymmetrical hardness profile shown in Fig. 3 it is obvious that more heat is generated on the RS of the weld compared to the advancing side (AS). This is believed to reflect the pertinent differences in the tool force acting on the respective sides during pin rotation. Similar observations have also been made for FSW (Liu and Ma, 2008, Zhang *et al.*, 2014).

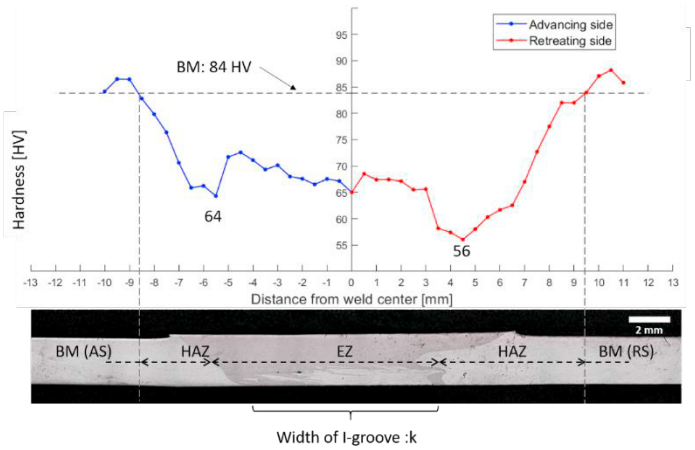

Fig. 3. Measured transverse hardness profile and optical macrograph of the 2 mm AA6060-T6 HYB joint cross-section. Note that the horizontal heavy broken line in the macrograph indicates the approximate position below the plate surface where the hardness measurements have been conducted. In this plot each hardness point represent the mean value of three individual measurements.

3.2. Tensile properties

Fig. 4 shows graphical representations of the tensile test data obtained for the different series. Note that the subscript *red* refers the specimens with a reduced thickness, whereas the error bars in the graphs represent the standard deviation

of three individual measurements for each set. It is evident from Fig. 4(a) that both the yield strength and the tensile strength of the as-welded samples (i.e. EZ, EZ_{red}, HAZ and HAZ_{red}) are significantly lower than the corresponding measured values for the BM. The highest weld zone yield strength is found for the EZ_{red} specimens, which display an average value of 146 MPa. This is comparable to that reported previously for AA6082-T6 HYB weldments (Sandnes *et al.*, 2018). Moreover, it is interesting to note that neither the specimen location nor the specimen thickness seems to affect the measured yield or tensile strength significantly. This essentially means that the previously mentioned "kissing" bond is not devastating for the resulting tensile properties. The same is also true when it comes to the tensile ductility, as shown by the fracture strain data presented in Fig. 4(b). All weld zones reveal an acceptable tensile ductility, although the values do not fully match the measured fracture strain of the BM specimens. This is to be expected, since the weld samples have been exposed to considerably strain localization and necking prior to fracture because of the associated EZ and HAZ softening.

After tensile testing the broken specimens were visually examined. Whereas all EZ_{red} specimens with a reduced thickness fractured in the soft zone on the AS of the joint, the corresponding EZ specimens with full thickness fractured in the soft zone on the RS (i.e. on the same side as the "kissing" bond location). As a matter of fact, all other specimens sampling the HAZ did fracture on the RS of the joint regardless of the specimen thickness. This observation is not surprising, considering the fact that the minimum HAZ hardness is seen to be located on the RS, as shown previously in Fig. 3.

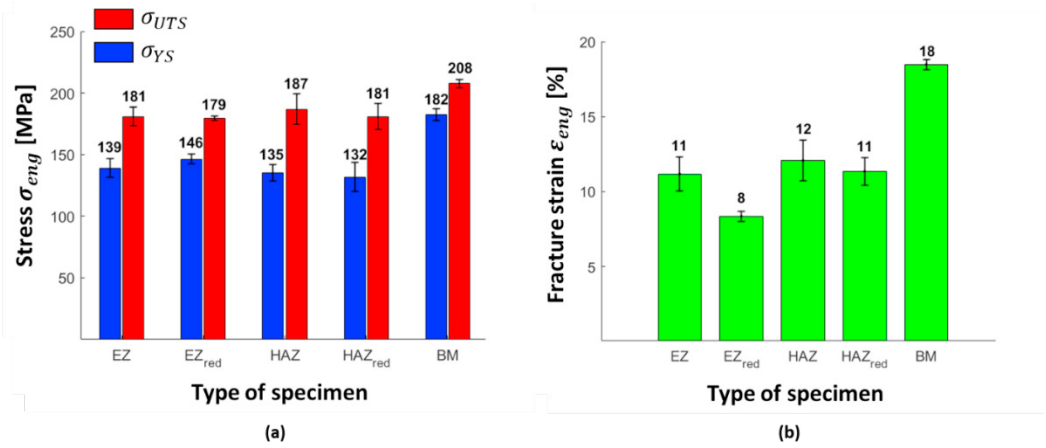

Fig. 4. Measured tensile properties for different regions of the 2 mm AA6060-T6 HYB joint, i.e. the Extrusion Zone (EZ), the Heat-Affected Zone (HAZ) and the base material (BM); (a) Offset yield strength (YS) and tensile strength (UTS), (b) Fracture strain. Note that the error bars in the graphs represent the standard deviation of the measurements, while subscript *red* refers to specimens having a reduced thickness.

4. Discussion

In the following, attempts will be made to explain the observed tensile properties of the 2 mm AA6060-T6 HYB butt joint and, in particular, why the yield and tensile strengths in the as-welded condition are so high, exceeding 135 and 180 MPa, respectively. As a matter of fact, these values are comparable with those reported for FSW of 2 mm AA6082-T6 profiles (Arab *et al.*, 2018) and surpass those reported for FSW of 2 mm AA6061-T6 profiles as far as the yield strength is concerned (Astarita *et al.*, 2016).

4.1. Weld softening in the context of engineering design

Traditionally, the 1 inch (25 mm) thumb rule has been applied to predict the soft zone width in aluminum welds (Mazzolani, 1995, Hagström and Sandström, 1997), which is very conservative particularly when it comes to thin walled extrusions and sheet materials (Astarita *et al.*, 2016, Arab *et al.*, 2018). Therefore, some design codes have opened up for a more specific (or graded) treatment by recommending different combinations of the minimum strength

level σ_{min} and the reduced strength zone Δy_{red} width for such weldments (Myhr and Grong, 2009). Unfortunately, the design codes are mutually inconsistent in the sense that they contribute to confusion about the numerical values of σ_{min} and Δy_{red} and how different alloy variants respond to welding and HAZ softening.

In the past, several investigators have addressed this inconsistency and pointed out a direction which can be followed to allow for individual differences between dissimilar alloys, section sizes, welding parameters and methods when calculating the design stress and resulting load bearing capacity of aluminum joints (Myhr and Grong, 2009). The approach undertaken here is based on Mazzolini's design methodology and his definition of the equivalent width of the reduced strength zone Δy_{red} (Mazzolani, 1995), where the actual strength profile across the weld zone is taken into consideration in the computation. By combining this methodology with a mechanical model and ABAQUS simulations, it is possible to obtain a verified quantitative understanding of the key factors contributing to the observed tensile properties of the 2 mm AA6060-T6 HYB butt joint.

4.2. Outline of the mechanical model

As a starting point, the measured HAZ hardness profile in Fig. 3 is converted into an equivalent yield strength profile using the well-established relationship between hardness (HV) and yield strength (σ_{ys}) for Al-Mg-Si alloys (Myhr and Grong, 1991, Grong, 1997):

$$\sigma_{ys} = 3.0HV + 48.1 \tag{1}$$

The resulting yield strength profile is shown in Fig. 5. From this graph the following values for the equivalent reduced strength zone width of the EZ and the HAZ can be read off:

$$\Delta y_{red}^{eq}(EZ)\text{: } 10.5\ mm, \qquad \Delta y_{red}^{eq}(HAZ)\text{: } 4\ mm$$

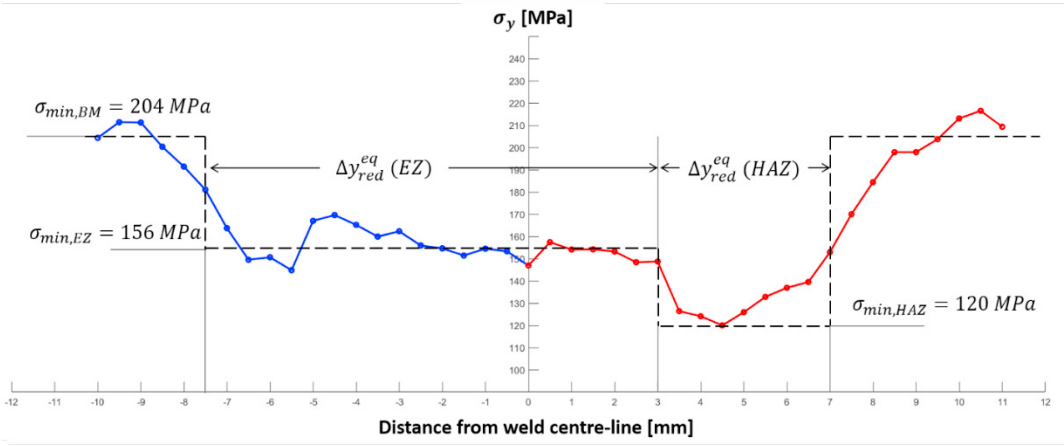

Fig. 5. Calculated transverse yield strength profile across the 2 mm AA6060-T6 HYB butt joint. Included in the graph are also the equivalent reduced strength zone widths of the EZ and the HAZ.

The next step is to develop a simple strength model for the EZ by assuming that its properties are a mix of those of the soft HAZ material and the harder FM. The area (and volume) fraction f_{FM} of the FM inside the EZ can be estimated from the value given above for the $\Delta y_{red}^{eq}(EZ)$ and the applied groove width k, which is a process parameter determining the extent of the FM addition in the HYB case. Taking $k = 7.5\ mm$, we obtain:

$$f_{FM} = \frac{k}{\Delta y_{red}^{eq}} = \frac{7.5}{10.5} = 0.71 \tag{2}$$

This rough estimate shows that the EZ, according to the reduced strength zone definition in Fig. 5, consists of 71% FM and 29% soft HAZ material.

4.3. Input data used in the FE simulations

Implementation of the mechanical model in ABAQUS requires relevant true stress-strain curves for both the T6-heat treated BM, the soft HAZ material and the FM. The necessary input data for the BM have been derived from the tensile results obtained in the present investigation, whereas the corresponding data for the soft HAZ material and the FM are taken from two independent sources (Myhr *et al.*, 2009, SINTEF, 2018). Fig. 6 contains graphical representations of the assembled true stress-strain curves, which are well-described by the following variant of Ludwik's law:

$$\sigma = \sigma_{ys} + K\varepsilon_p^n \tag{3}$$

where σ is the true stress, σ_{ys} is the stress at the on-set yielding, ε_p is the true plastic strain, while K and n are fitting parameters. Table 4 summarizes the main input data, including the relevant values for σ_{ys}, K and n for the BM, the soft HAZ material and the FM.

Table 4. Summary of the input data used to calculate the true stress-strain curves for the BM, the soft HAZ material and the FM from Ludwik's law.

	σ_{ys} (MPa)	K (MPa))	n	Source
BM	182	360.9	0.72	Present investigation
HAZ	100	194.5	0.33	(Myhr *et al.*, 2009)
FM	186.5	453.3	0.62	(SINTEF, 2018)

To obtain the true stress-strain cure for the EZ, we first invoke the "rule of mixtures" (Callister and Rethwisch, 2007), which in the past also has been successfully applied to predict the mechanical properties of dissimilar welds (Abdullah *et al.*, 2001). Then the next step is to assume that the EZ can be treated as a composite material, where the true stress σ_{EZ} acting on an element during loading, at any strain, is given by the weighted average of the true stress acting on each of its components σ_{FM} and σ_{HAZ}:

$$\sigma_{EZ} = f_{FM}\,\sigma_{FM} + (1 - f_{FM})\,\sigma_{HAZ} \tag{4}$$

where σ_{FM} and σ_{HAZ} refer to the true stress in the FM and the soft HAZ material, respectively, as calculated from Equation 3.

It follows from Equation 4 that the true stress-strain curve for the EZ is determined by the actual value of f_{FM} and can therefore vary within wide limits, depending on the operational conditions applied. Fig. 6 includes a plot of the predicted stress-strain curve for the EZ at $f_{FM} = 0.71$, which refers back to the present experimental set-up and a groove width k of 7.5 mm.

4.4. Validation of the FE model

Fig. 7 shows a comparison between measured (solid line) and simulated (dashed line) engineering stress-strain curves for the 2 mm AA6060-T6 HYB butt weld following implementation of the mechanical model in ABAQUS. As can be seen from the figure, the FE model gives a fair representation of the mechanical response during tensile testing, showing that the simulation set-up is sound and the applied input data reasonable in the content of the model being developed. This justifies further use of the FE model to re-assess the previously reported tensile test results in Fig. 4 and evaluate how the yield strength values achieved depend on the applied specimen geometry.

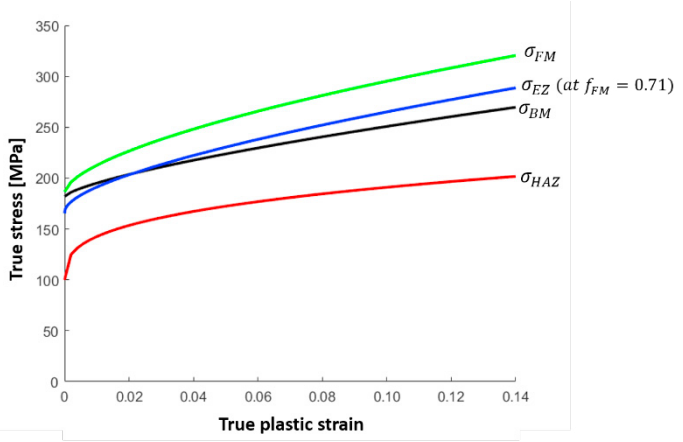

Fig. 6. Graphical representations of the assembled true stress-strain curves for the BM, the soft HAZ material and the FM. These have been calculated from Equation 3, using input data from Table 4. Included is also the corresponding stress-strain curve for the EZ at $f_{FM} = 0.71$.

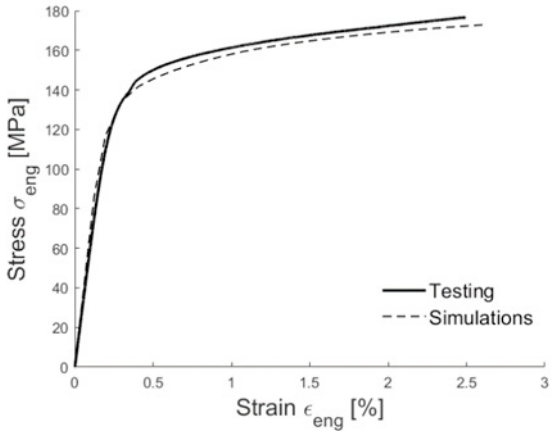

Fig. 7. Comparison between simulated (dashed line) and measured (solid line) engineering stress-strain curves for the 2 mm AA6060-T6 HYB butt joint.

4.5. Re-assessment of the tensile test results

It has previously been notified that the measured yield strength data in Fig. 4 may be affected by the use of a short gauge length in cases where the extensometer does not fully sample the entire width of the soft HAZ. The situation is most critical for the EZ tensile specimens, as shown in Fig. 8(a), because the early strain localization occurring in the soft HAZ on the RS of the weld is only partly recorded by the extensometer. Therefore, the measured yield strength values referring back to the EZ specimens are probably too high. On the other hand, the use of a short gauge length is not a problem for the HAZ tensile specimens, as illustrated in Fig. 8(b), since the soft HAZ in that case is located in the middle of the extensometer. Hence, these values are deemed to be representative of the actual yield strength of the 2 mm AA6060-T6 HYB butt weld and should thus be used as a basis for comparison with FSW.

Table 5 summarizes the tensile test results obtained in the present investigation along with those reported for FSW of 2 mm profiles of the high strength AA6082-T6 and AA6061-T6 grades. Obviously, the tensile properties of the 2 mm AA6060-T6 HYB joint are comparable with those of the FS welds, even after the yield strength correction.

Table 5. Summary of tensile test results obtained following HYB and FSW of 2 mm profiles of different Al-Mg-Si alloys.

Material	Welding process	Total width of weld zone (mm)	σ_{ys} (MPa)	σ_{UTS} (MPa)	Welding speed (mm/s)	Pin rotation (RPM)	Source
AA6082-T6	FSW	27	140	203	1.3	1400	(Arab *et al.*, 2018)
AA6082-T6	FSW	22	146	188	1.3	500	(Arab *et al.*, 2018)
AA6061-T6	FSW	16	113	202	1.3	900	(Astarita *et al.*, 2016)
AA6060-T6	HYB	18	134*	182**	8	250	Fig. 4

* Average of the two HAZ specimens

** Average of all tensile specimens

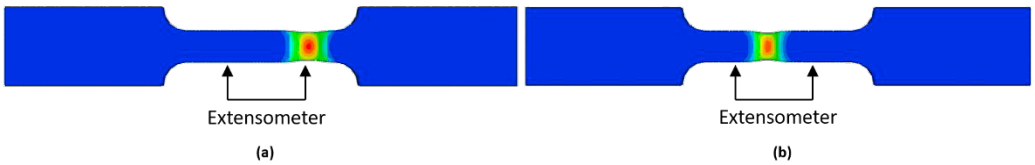

Fig. 8. ABAQUS simulations of the experimental set-up during tensile testing; (a) Strain distribution across the EZ tensile specimen centered in the middle of the weld, (b) Strain distribution across the HAZ tensile specimen centered in the soft zone on the retreating side (RS) of the weld.

5. Conclusions

It is confirmed that the previously observed "kissing" bond formation on the retreating side (RS) of the 2 mm AA6060-T6 HYB butt weld is not devastating for the resulting tensile properties. On the average, the actual yield and tensile strength in the as-welded condition was found to be 134 and 182 MPa, respectively.

Generally speaking, the use of a lean aluminum alloy with a low base material (BM) strength will inevitably reduce the significance of the Heat-Affected Zone (HAZ) softening during welding. This is because the drop in strength following dissolution of the BM hardening precipitates will be correspondingly small. The low initial strength of the AA6060-T6 BM explains the extraordinarily high yield and tensile strength joint efficiencies of 74% and 88%, respectively being observed in the present case.

In the HYB case, where joining occurs by filler metal (FM) addition in the solid state, the weld can be sub-divided into two distinct zones, i.e. the Extrusion Zone (EZ) and the HAZ. The tensile properties of the EZ are a mix of those of the soft HAZ material and the harder FM. Thus, by treating the EZ as a composite material, the mechanical response can be calculated from a "rule of mixtures" by assuming that the true stress acting on an element during loading, at any strain, is given by the weighted average of the true stress acting on each of its components.

Following the implementation of this mechanical model in ABAQUS, the observed stress-strain response of the 2 mm AA6060-T6 HYB butt weld has been fully reproduced and rationalized. The same finite element (FE) model is then employed for re-assessment of the tensile test experimental set-up and the measured yield strength values. Even after correcting for the use of a non-standardized specimen geometry which brings uncertainty to some of the readings, the actual tensile properties of the HYB joint are comparable with those reported for FSW of 2 mm AA6082-T6 profiles and surpass those reported for FSW of 2 mm AA6061-T6 profiles as far as the yield strength is concerned. This is because of the unique properties of the AA6082 FM, which reduces the significance of the HAZ softening within the EZ.

Acknowledgements

The authors acknowledge the financial support from HyBond AS, NTNU and NAPIC (NTNU Aluminum Product Innovation Center). They are also indebted to Ulf Roar Aakenes and Tor Austigard of HyBond AS for valuable assistance in producing the 2 mm AA6060-T6 HYB joint being examined in the present investigation.

References

Abdullah, K., Wild, P. M., Jeswiet, J. J. and Ghasempoor, A., 2001. Tensile testing for weld deformation properties in similar gage tailor welded blanks using the rule of mixtures. Journal of Materials Processing Technology 112, 91-97.

Arab, M. A., Zemri, M. and Blaoui, M. M., 2018. Experimental Investigation on the Effect of Tool Rotational Speed on Mechanical Properties of AA6082-T6 Friction Stir-Welded Butt Joints. Journal of Failure Analysis & Prevention 18, 1625-1630.

Astarita, A., Squillace, A. and Nele, L., 2016. Mechanical Characteristics of Welded Joints of Aluminum Alloy 6061 T6 Formed by Arc and Friction Stir Welding. Metal Science and Heat Treatment 57, 564-569.

Bruce, G. J. and Eyres, D. J., 2012. Welding Distortions. in "*Ship Construction (7th Edition)*". Oxford, Elsevier.

Callister, W. D. and Rethwisch, D. G., 2007. Materials science and engineering (9th Edition). John Wiley & Sons New York.

Davis, J. R., 1993. Aluminum and aluminum alloys. Materials Park, OH, ASM international.

Farajkhah, V., Liu, Y. and Gannon, L., 2017. Finite element study of 3D simulated welding effect in aluminium plates. Ships and Offshore Structures 12, 196-208.

Frigaard, Ø., Grong, Ø. and Midling, O. T., 2001. A process model for friction stir welding of age hardening aluminum alloys. Metallurgical and Materials Transactions A 32, 1189-1200.

Grong, Ø., 1997. Metallurgical modelling of welding. 2. London, UK, Institute of Materials.

Grong, Ø., Sandnes, L., Bergh, T., Vullum, P. E., Holmestad, R. and Berto, F., 2019. An analytical framework for modelling intermetallic compound (IMC) formation and optimising bond strength in aluminium-steel welds. Material Design & Processing Communications 1, e57.

Grong, Ø., Sandnes, L. and Berto, F., 2019. A Status Report on the Hybrid Metal Extrusion & Bonding (HYB) Process and Its Applications. Material Design & Processing Communications 1, e41.

Hagström, J. and Sandström, R., 1997. Mechanical properties of welded joints in thin walled aluminium extrusions. Science Technology of Welding Joining 2, 199-208.

Hatch, J. E., 1984. Aluminum - Properties and Physical Metallurgy. Materials Park, OH, American Society for Metals.

Hirsch, J., 2011. Aluminium in innovative light-weight car design. Materials Transactions 52, 818-824.

Huang, Y., Wan, L., Huang, T., Lv, Z., Zhou, L. and Feng, J., 2016. The weld formation of self-support friction stir welds for aluminum hollow extrusion. The International Journal of Advanced Manufacturing Technology 87, 1067-1075.

Kumar, R., Dilthey, U., Dwivedi, D. K., Sharma, S. P. and Ghosh, P. K., 2008. Welding of thin sheet of Al alloy (6082) by using Vario wire DC P-GMAW. The International Journal of Advanced Manufacturing Technology 42, 102-117.

Liu, F. and Ma, Z., 2008. Influence of tool dimension and welding parameters on microstructure and mechanical properties of friction-stir-welded 6061-T651 aluminum alloy. Metallurgical and Materials Transactions A 39, 2378-2388.

Ma, Z. Y., Feng, A. H., Chen, D. L. and Shen, J., 2018. Recent Advances in Friction Stir Welding/Processing of Aluminum Alloys: Microstructural Evolution and Mechanical Properties. Critical Reviews in Solid State and Materials Sciences 43, 269-333.

Mazzolani, F. M., 1995. Aluminium alloy structures. 2nd. London, E & FN Spon.

Myhr, O., Grong, O., Lademo, O. and Tryland, T., 2009. Optimizing Crash Resistance of Welded Aluminum Structures. Welding Journal 88, 42-45.

Myhr, O. and Grong, Ø., 1991. Process modelling applied to 6082-T6 aluminium weldments—II. Applications of model. Acta Metallurgica et Materialia 39, 2703-2708.

Myhr, O. and Grong, Ø., 2009. Novel modelling approach to optimisation of welding conditions and heat treatment schedules for age hardening Al alloys. Science and technology of welding and joining 14, 321-332.

Sandnes, L., Grong, Ø., Torgersen, J., Welo, T. and Berto, F., 2018. Exploring the hybrid metal extrusion and bonding process for butt welding of Al–Mg–Si alloys. The International Journal of Advanced Manufacturing Technology 98, 1059-1065.

Sandnes, L., Romere, L., Berto, F., Welo, T. and Grong, Ø., 2019. Assessment of the Mechanical Integrity of a 2 mm AA6060-T6 Butt Weld Produced Using the Hybrid Metal Extrusion & Bonding (HYB) Process –Part I: Bend Test Results. Procedia Manufacturing, 47th North American Manufacturing Research Conference (NAMRC47), Pennsylvania, USA.

SINTEF, 2018. Hardness measurements and tensile testing of all-weld HYB specimens, Trondheim, Norway.

Wanjara, P., Monsarrat, B. and Larose, S., 2013. Gap tolerance allowance and robotic operational window for friction stir butt welding of AA6061. Journal of Materials Processing Technology 213, 631-640.

Zha, Y. and Moan, T., 2001. Ultimate strength of stiffened aluminium panels with predominantly torsional failure modes. Thin-Walled Structures 39, 631-648.

Zhang, Z., Xiao, B. L. and Ma, Z. Y., 2014. Hardness recovery mechanism in the heat-affected zone during long-term natural aging and its influence on the mechanical properties and fracture behavior of friction stir welded 2024Al–T351 joints. Acta Materialia 73, 227-239.